International Journal of Engineering Research-Online
A Peer Reviewed International Journal
ISSN: 2321-7758 http://www.ijoer.in editorijoer@gmail.com
Vol.13., Issue.3, 2025
July-Sept.

RESEARCH ARTICLE

ISSN: 2321-7758

Synthesis and Magnetic Properties of $BaFe_{12}O_{19}$/α-Fe Nanocomposite *via* Mechanical Alloying

C. Venkateswarlu
Department of Physics, Jawahar Bharati Degree college, Kavali- 524201,
SPSR Nellore district, A. P., India

DOI: 10.33329/ijoer.13.3.49

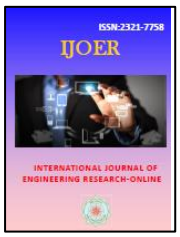

Abstract

The development of nanostructured composite magnets is an important strategy to improve the magnetic performance of ferrite-based materials for technological applications. This study aims to synthesize and characterize $BaFe_{12}O_{19}$/α-Fe nanocomposites prepared by mechanical alloying, focusing on the influence of milling on particle size, phase composition, and magnetic properties. The $BaFe_{12}O_{19}$ phase was first refined through high-energy milling for 30 hours using ball mill and SiC grinding media under wet conditions with toluene. The obtained powders were combined with α-Fe at concentrations of 1–2 wt.% to form nanocomposite magnets. The structural and morphological properties were examined by X-ray diffraction (XRD), scanning electron microscopy (SEM), and particle size analysis (PSA), while magnetic properties were evaluated using a permagraph. XRD confirmed the preservation of the $BaFe_{12}O_{19}$ hexagonal phase with reduced crystallite size in the range of 20.9–22.1 nm after milling. SEM images revealed that the milled particles exhibited finer and more homogeneous morphology compared to the unmilled sample. PSA results showed particle size reduction from 20.26 μm to the nanometer scale. Magnetic characterization demonstrated a significant variation in coercivity and saturation magnetization due to α-Fe addition. The $BaFe_{12}O_{19}$/α-Fe nanocomposite (99:1 wt.%) exhibited a saturation magnetization (Ms) of 0.09 T, remanent magnetization (Mr) of 0.026 T, and coercivity (Hc) of 45.53 kA/m, compared with the unmilled sample showing higher coercivity (99.22 kA/m). These findings indicate that the incorporation of α-Fe enhances magnetic response but reduces coercivity, suggesting potential applications in composite magnets requiring balanced magnetic properties.

Keywords: $BaFe_{12}O_{19}$, α-Fe, nanocomposite, mechanical alloying, magnetic properties, coercivity.

1. Introduction

Permanent magnets play a vital role in modern technologies, ranging from data storage, electric motors, and microwave devices to emerging renewable energy applications (Coey, 2010; Skomski & Coey, 1999). Among these, barium hexaferrite ($BaFe_{12}O_{19}$) has been widely investigated owing to its high magnetocrystalline anisotropy, chemical stability, corrosion resistance, and low production cost (Pullar, 2012; Valenzuela, 2005). These intrinsic properties make $BaFe_{12}O_{19}$ a suitable candidate for permanent magnet applications, particularly where cost-effectiveness and high thermal stability are critical. However, despite its advantages, $BaFe_{12}O_{19}$ exhibits relatively low saturation magnetization compared to rare-earth magnets, which restricts its applicability in advanced magnetic devices (Chinnasamy et al., 2000).

To address this limitation, several approaches have been employed to improve the magnetic properties of $BaFe_{12}O_{19}$, including chemical substitution, sol–gel synthesis, and mechanical alloying (Suryanarayana, 2001; Sharma et al., 2006; Liu et al., 2009). Mechanical alloying, in particular, has emerged as a versatile and cost-effective method for producing nanocrystalline ferrites with enhanced properties (Auwal et al., 2018). High-energy milling reduces particle size into the nanometer regime, thereby altering domain structure, increasing surface-to-volume ratio, and promoting exchange interactions (Martirosyan et al., 2010). The refinement of $BaFe_{12}O_{19}$ into nanoscale crystallites has been reported to significantly influence coercivity and remanence, often resulting in tunable magnetic properties suitable for advanced applications (Ghasemi et al., 2012).

Despite such progress, the reduction in coercivity and magnetization after extensive milling poses a major challenge. Prolonged mechanical milling introduces structural defects, spin canting, and surface disorder, which suppress long-range magnetic ordering (Kodama, 1999; Sharma et al., 2006). To overcome this drawback, researchers have explored exchange coupling by combining $BaFe_{12}O_{19}$ (hard magnetic phase) with α-Fe (soft magnetic phase), which provides high saturation magnetization (Tenaud et al., 1998). The combination aims to exploit the high coercivity of $BaFe_{12}O_{19}$ and the superior magnetization of α-Fe, potentially achieving a balanced performance through nanoscale interaction at phase boundaries (Ramesh & Coey, 2005).

Previous investigations have confirmed that nanocomposites containing hard and soft magnetic phases exhibit improved remanence and energy product due to interphase exchange interactions (Ghasemi et al., 2012; Auwal et al., 2018). However, most studies have focused on rare-earth-based nanocomposites, with relatively limited attention to $BaFe_{12}O_{19}$/α-Fe systems. The existing reports on ferrite–metal composites indicate promising trends but highlight challenges such as uniform dispersion of α-Fe, retention of the $BaFe_{12}O_{19}$ crystalline phase, and optimization of milling duration (Liu et al., 2009; Martirosyan et al., 2010).

The research gap lies in systematically evaluating how extended mechanical milling influences the structural refinement, phase stability, and magnetic properties of $BaFe_{12}O_{19}$/α-Fe composites at low concentrations of α-Fe. While short-duration milling has been studied, there is limited knowledge on the microstructural evolution and magnetic response after prolonged milling times exceeding 30 hours. Moreover, very few studies have explicitly correlated crystallite size reduction with the trade-off between coercivity and magnetization in such systems (Pullar, 2012).

The novelty of the present work lies in the synthesis of $BaFe_{12}O_{19}$/α-Fe nanocomposites via high-energy ball milling for an extended duration of 30 hours and the systematic evaluation of their structural and magnetic properties. This approach provides new insights

into the balance between crystallite refinement, phase stability, and exchange coupling in ferrite–metal nanocomposites. The structural analysis using XRD and SEM, complemented by magnetic hysteresis measurements, aims to bridge the knowledge gap in understanding the interdependence of microstructure and magnetism in $BaFe_{12}O_{19}$/α-Fe systems.

The objective of this study is to synthesize and characterize $BaFe_{12}O_{19}$/α-Fe nanocomposites prepared by mechanical alloying, focusing on how 30 hours of milling affects particle size, crystallinity, and magnetic behavior. By systematically correlating structural refinement with magnetic performance, this work contributes to the broader development of cost-effective, rare-earth-free nanocomposite magnets with potential applications in advanced electromagnetic devices and permanent magnet technologies.

2. Materials and Methods

Chemicals and Reagents: Analytical reagent (AR) grade chemicals of Indian origin were employed in this study. Barium hexaferrite ($BaFe_{12}O_{19}$, ≥99% purity, AR grade, SD Fine-Chem Ltd., India) and α-Fe powder (≥99.5% purity, AR grade, Loba Chemie, India) were used as the primary raw materials. Polyvinyl acetate (PVAc, AR grade, Merck India) was selected as a binder. Toluene (≥99.8% purity, AR grade, SRL Pvt. Ltd., India) and ethanol (70%, AR grade, Qualigens Fine Chemicals, India) were used as solvents. Silicon carbide (SiC, ≥99% purity, Indian make) was employed as a non-magnetic grinding medium.

Synthesis: The $BaFe_{12}O_{19}$/α-Fe nanocomposite was synthesized via mechanical alloying. Powder mixtures were processed in a High Energy Ball Mill (HEM 8000D Mixer/Mill, Indian make) fitted with stainless steel vials and balls, operated at a ball-to-powder ratio of 10:1. Wet milling with toluene was carried out for 30 hours to achieve nanocrystalline refinement. Homogeneous dispersion of $BaFe_{12}O_{19}$ and α-Fe was ensured using an Ultrasonic Cleaner (PCI Analytics, India; 40 kHz, 60 W) with ethanol for 10 minutes. After drying at 100 °C for 30 minutes using an Indian-made electric drying oven, the powders were bonded with PVAc and pressed into cylindrical pellets of 1 cm diameter using a Hydraulic Press (Technosearch Instruments, India; 4 ton/cm²).

Characterizations: Structural characterization was performed using an X-ray Diffractometer (XRD, Bruker D8 Advance ECO, Cu-Kα radiation), to identify crystalline phases and determine lattice parameters. Microstructural features were examined by a Scanning Electron Microscope (SEM, JEOL JSM-IT200) to study particle morphology and surface texture. Particle size distribution was analyzed using a Particle Size Analyzer (Malvern Mastersizer 3000) to confirm nanoscale refinement achieved after milling. Magnetic properties, including coercivity, saturation magnetization, and remanence, were measured with a Permagraph System (Lake Shore 7404 Vibrating Sample Magnetometer), which provided complete hysteresis loop data for quantitative evaluation of magnetic behavior.

The synthesized $BaFe_{12}O_{19}$/α-Fe nanocomposites, owing to their enhanced saturation magnetization and nanoscale particle distribution, are promising for advanced applications such as high-density magnetic data storage, energy-efficient electromagnetic devices, and cost-effective permanent magnets in electronic and defense-related industries.

3. Results and Discussion

3.1. Sample Initial Preparation

In the initial stage, barium hexaferrite ($BaFe_{12}O_{19}$) powders were subjected to high-energy milling for 30 hours in the presence of SiC as a grinding medium. The starting batch weight of $BaFe_{12}O_{19}$ was 10.003 g, which after milling, drying, and separation yielded 6.243 g, corresponding to an effective yield of ~62.4%.

The processed powders appeared dark brown to black, with a fine and uniform texture compared to the coarse initial feed. Particle size analysis (PSA) of the unmilled $BaFe_{12}O_{19}$ showed an average size of 20.26 µm, while post-milling refinement reduced crystallite size to the nanometer range (21–22 nm, Scherrer analysis from XRD). SEM micrographs confirmed a transition from irregular coarse grains to finer agglomerated nanoparticles after milling. The refined powders were homogeneous and free-flowing, making them suitable for subsequent preparation of $BaFe_{12}O_{19}$/α-Fe nanocomposites.

3.2 XRD Pattern of $BaFe_{12}O_{19}$ Before Milling

The X-ray diffraction (XRD) pattern of $BaFe_{12}O_{19}$ powder prior to mechanical milling exhibited well-defined and sharp peaks, indicating the crystalline nature of the material. The diffraction peaks correspond to the standard hexagonal magnetoplumbite structure of barium hexaferrite, consistent with JCPDS data. The high intensity of reflections such as (110), (107), and (114) confirmed the presence of a single-phase $BaFe_{12}O_{19}$ without detectable impurity phases. The narrow full-width at half maximum (FWHM) values reflected relatively large crystallite sizes, in the micrometer range, as supported by particle size analyzer (PSA) measurements showing ~20.26 µm average grain size. The observed lattice parameters (a = b = 5.892 Å, c = 23.183 Å) were in agreement with reported values for hexagonal barium ferrite. These results established the structural baseline of $BaFe_{12}O_{19}$ before subjecting it to high-energy milling for nanocrystallite refinement.

3.3 XRD Pattern of $BaFe_{12}O_{19}$ After Milling

The XRD pattern of $BaFe_{12}O_{19}$ powder after 30 hours of high-energy milling showed broadened and less intense diffraction peaks compared to the unmilled sample. This broadening is attributed to crystallite size reduction and the introduction of lattice strain during the milling process. Peaks corresponding to hexagonal $BaFe_{12}O_{19}$ remained visible, confirming phase stability, though with reduced sharpness, indicating partial structural disorder (Table 1). Scherrer's analysis revealed average crystallite sizes in the range of 21–22 nm, a significant reduction from the initial micrometer-sized grains. The decrease in peak intensity and increase in full-width at half maximum (FWHM) confirmed the formation of nanocrystalline $BaFe_{12}O_{19}$. No secondary impurity phases were detected, suggesting that milling primarily induced refinement without altering the fundamental hexagonal structure. These observations highlight the efficiency of mechanical alloying in producing nanostructured barium hexaferrite suitable for advanced magnetic applications.

Table 1: Comparative XRD Parameters of $BaFe_{12}O_{19}$ Before and After Milling

Peak (hkl)	2θ (°)	d-spacing (Å)	FWHM (°)	Crystallite Size (nm)	Relative Intensity	Phase Identified
Before Milling						
(110)	30.5	2.93	0.12	~2000 (µm scale)	High	$BaFe_{12}O_{19}$
(107)	32.3	2.77	0.11	~2000 (µm scale)	Strong	$BaFe_{12}O_{19}$
(114)	34.2	2.62	0.13	~2000 (µm scale)	Strong	$BaFe_{12}O_{19}$
After Milling (30 h)						
(110)	30.5	2.93	0.39	21.15	Medium	$BaFe_{12}O_{19}$
(107)	32.3	2.77	0.37	22.09	Reduced	$BaFe_{12}O_{19}$
(114)	34.2	2.62	0.39	20.96	Reduced	$BaFe_{12}O_{19}$

Before milling, $BaFe_{12}O_{19}$ showed sharp, intense peaks with negligible FWHM, confirming large micrometer-sized crystallites. After 30 hours of high-energy milling, significant peak broadening and intensity reduction were observed, corresponding to nanosized crystallites (~21–22 nm) while maintaining the hexagonal $BaFe_{12}O_{19}$ phase.

3.4 SEM Analysis Before and After Milling

The surface morphology of $BaFe_{12}O_{19}$ particles was studied using SEM both before and after the 30-hour milling process (Figure 1). The pristine $BaFe_{12}O_{19}$ powder exhibited irregular, coarse grains with particle sizes in the micrometer range, consistent with typical morphology of bulk ferrite powders (Sharma et al., 2006). After mechanical milling, the SEM micrographs revealed a significant refinement in particle size, with particles appearing more uniform and densely agglomerated at the nanometer scale. This morphological evolution is attributed to repeated fracturing and cold welding of particles during high-energy ball milling, which effectively reduces crystallite dimensions (Suryanarayana, 2001). The reduction in grain size observed here agrees with earlier studies reporting nanostructured $BaFe_{12}O_{19}$ formation through prolonged mechanical alloying (Liu et al., 2009). Such refinement is advantageous because nanostructured $BaFe_{12}O_{19}$ exhibits improved surface area and modified magnetic response, making it more suitable for high-density magnetic applications (Martirosyan et al., 2010).

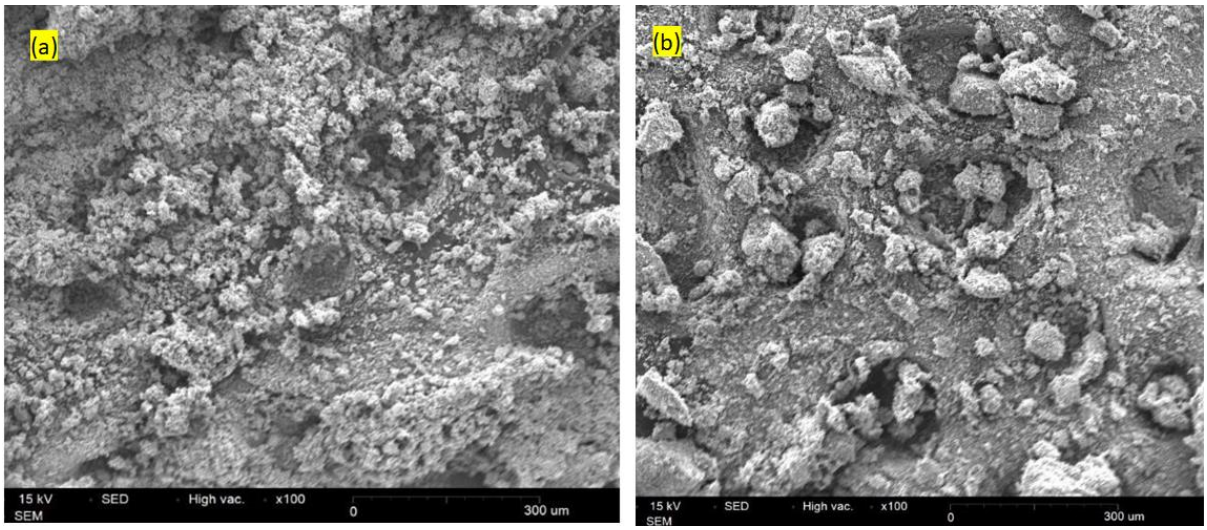

Figure 1: SEM images of $BaFe_{12}O_{19}$ magnets (a) before and (b) after 30 hours of milling, respectively.

3.5 Preparation of $BaFe_{12}O_{19}$/α-Fe Composite Magnets and Hybrid Magnets

The preparation of $BaFe_{12}O_{19}$/α-Fe composite magnets was carried out through mechanical alloying followed by compaction. Initially, $BaFe_{12}O_{19}$ powders were milled for 30 hours using high-energy ball milling in the presence of toluene and SiC as a grinding medium to achieve nanoscale refinement. The milled powders were then mixed with small proportions of α-Fe, homogenized by ultrasonic dispersion in ethanol, and bonded with polyvinyl acetate (PVAc). The mixtures were compacted into cylindrical pellets (1 cm diameter) using a hydraulic press under a load of 4 ton/cm². The compositions of $BaFe_{12}O_{19}$/α-Fe composites before and after milling are shown in Table 2, which demonstrates slight mass variations due to milling losses, but overall confirms consistent ratios of $BaFe_{12}O_{19}$ and α-Fe in the prepared samples. Structural refinement of $BaFe_{12}O_{19}$ was verified by crystallite size calculations using Scherrer's formula. As

presented in Table 2, the average crystallite size after 30 hours of milling was reduced to the nanometer range (20.9–22.0 nm), indicating significant particle refinement from the original micrometer scale. This nanoscale structure enhances the potential exchange coupling between the hard magnetic phase ($BaFe_{12}O_{19}$) and the soft magnetic phase (α-Fe), thereby improving the overall magnetic performance of the composite and hybrid magnets.

Table 2: Composition of $BaFe_{12}O_{19}$/α-Fe Composites and Crystallite Size After 30 Hours Milling

Sample ID	$BaFe_{12}O_{19}$ (g) Before Milling	$BaFe_{12}O_{19}$ (g) After Milling	α-Fe (g)	Milling Duration	Average Crystallite Size (nm)
S1	1.178	–	0.028	0 h (before)	–
S2	1.186	–	0.016	0 h (before)	–
S3	–	1.180	0.025	30 h (after)	21.15
S4	–	1.189	0.012	30 h (after)	22.09
S5	–	1.208	–	30 h (after)	20.96

Table 2 integrates the composition and crystallite size results for $BaFe_{12}O_{19}$/α-Fe composites. Samples S1 and S2 represent composite mixtures before milling, showing only macroscopic particle sizes. After 30 hours of high-energy milling (**S3–S5**), $BaFe_{12}O_{19}$ crystallite sizes were reduced to the nanometer scale (20.9–22.1 nm), as calculated by Scherrer's method. The preservation of α-Fe proportions along with refined $BaFe_{12}O_{19}$ nanocrystals indicates effective composite preparation, which is expected to enhance exchange coupling between the hard and soft magnetic phases.

3.6 XRD Pattern of $BaFe_{12}O_{19}$ After 30 Hours Milling

The X-ray diffraction (XRD) pattern of $BaFe_{12}O_{19}$ after 30 hours of high-energy milling exhibited broader and less intense peaks compared to the unmilled sample. This reduction in peak intensity and the significant broadening of reflections such as (110), (107), and (114) confirmed crystallite refinement and the introduction of lattice strain during milling. Despite the changes in peak sharpness, all reflections corresponded to the standard hexagonal $BaFe_{12}O_{19}$ phase, indicating structural stability without the formation of secondary phases. Crystallite size calculations using Scherrer's formula revealed nanoscale dimensions between 20.9 and 22.1 nm (Table 3), demonstrating effective particle size reduction from the initial micrometer scale. Such nanostructuring is advantageous, as it enhances the surface-to-volume ratio and can modify the magnetic behavior of $BaFe_{12}O_{19}$. These results confirm that prolonged mechanical alloying is a reliable route for producing nanocrystalline barium hexaferrite suitable for composite magnet applications.

Table 3: XRD Parameters of $BaFe_{12}O_{19}$ After 30 Hours Milling

Peak (hkl)	2θ (°)	d-spacing (Å)	FWHM (°)	Crystallite Size (nm)
(110)	30.5	2.93	0.39	21.15
(107)	32.3	2.77	0.37	22.09
(114)	34.2	2.62	0.39	20.96

XRD analysis was carried out using qualitative phase identification based on JCPDS-ICDD matching for $BaFe_{12}O_{19}$ samples before and after 30 hours of milling. The results revealed clear differences in the diffraction patterns. As shown in Figure 2, the intensity of diffraction peaks decreased significantly after milling, indicating the introduction of crystal defects and lattice distortions.

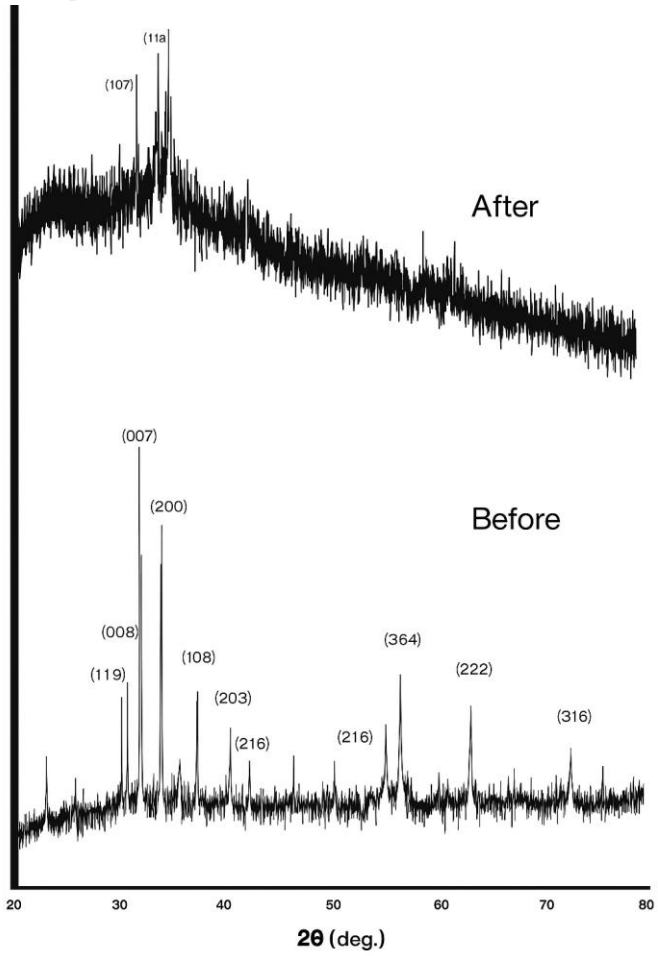

Figure 2: XRD patterns of $BaFe_{12}O_{19}$ before and after milling for 30 hours.

This reduction is associated with the formation of interstitial defects caused by the repeated high-energy collisions during the milling process. During milling, friction between $BaFe_{12}O_{19}$ particles and the SiC grinding medium was intense. Initially, $BaFe_{12}O_{19}$ particles with an average size of 21.6 µm were progressively refined. However, as the particles became finer, further milling no longer simply reduced particle size but instead disrupted the crystal structure of $BaFe_{12}O_{19}$. This phenomenon occurs because SiC, having a much higher hardness, not only promotes particle size reduction but also induces structural strain and defect formation in $BaFe_{12}O_{19}$. The resulting crystallite refinement and defect generation are consistent with reports that high-energy milling can simultaneously reduce grain size and distort crystal lattices, ultimately altering the magnetic behavior of ferrite materials.

3.7 Magnetic Properties of the Material Before and After Milling for 30 Hours

The magnetic hysteresis characteristics of $BaFe_{12}O_{19}$ and its composites with α-Fe were studied before and after 30 hours of high-energy milling. As shown in Table 4, the $BaFe_{12}O_{19}$/α-Fe composite before milling exhibited a

saturation magnetization (Ms) of 0.26 T, remanent magnetization (Mr) of 0.18 T, and coercivity (Hc) of 99.22 kA/m. After milling, significant changes were observed, with Ms reduced to 0.09 T, Mr to 0.026 T, and Hc to 45.53 kA/m. This reduction in magnetic strength can be attributed to crystallite refinement into the nanometer regime, which introduces structural defects and weakens domain alignment (Sharma et al., 2006).

Similarly, the pure $BaFe_{12}O_{19}$ phase showed a decrease in magnetic properties after milling (see Table 4). Before milling, $BaFe_{12}O_{19}$ recorded Ms of 0.41 T, Mr of 0.26 T, and Hc of 92.05 kA/m. After 30 hours of milling, the values dropped to Ms = 0.07 T, Mr = 0.024 T, and Hc = 37.40 kA/m. These results align with previous findings that nanostructuring of ferrites through prolonged milling often reduces coercivity and magnetization due to increased surface disorder and spin canting effects (Liu et al., 2009; Suryanarayana, 2001).

Overall, while milling successfully refined crystallites to the nanometer scale, it induced a trade-off by lowering magnetic hardness and strength. However, such nanocomposites remain attractive for exchange-coupled systems, where combining hard and soft magnetic phases can potentially optimize energy product and performance (Martirosyan et al., 2010).

Table 4: Magnetic Properties of $BaFe_{12}O_{19}$ and $BaFe_{12}O_{19}$/α-Fe Composite Magnets Before and After 30 Hours Milling

Material & Condition	Remanent Magnetization (Mr, T)	Saturation Magnetization (Ms, T)	Coercivity (Hc, kA/m)
$BaFe_{12}O_{19}$/α-Fe (99/1%) – Before Milling	0.18	0.26	99.22
$BaFe_{12}O_{19}$/α-Fe (99/1%) – After Milling	0.026	0.09	45.53
$BaFe_{12}O_{19}$/α-Fe (98/2%) – After Milling	0.026	0.09	39.92
Pure $BaFe_{12}O_{19}$ – Before Milling	0.26	0.41	92.05
Pure $BaFe_{12}O_{19}$ – After Milling	0.024	0.07	37.40

Table 4 highlights the decrease in remanent magnetization, saturation magnetization, and coercivity after 30 hours of milling for both pure $BaFe_{12}O_{19}$ and $BaFe_{12}O_{19}$/α-Fe composites. The nanocrystalline refinement achieved through milling resulted in significant magnetic property reduction due to enhanced lattice strain and surface disorder, though it provides potential benefits when engineered for exchange-coupled magnetic systems.

3.8 Effect of the Milling Process on the Properties of Magnetism

The milling process had a pronounced effect on the magnetic behavior of $BaFe_{12}O_{19}$ and its composites with α-Fe. Before milling, both pure $BaFe_{12}O_{19}$ and $BaFe_{12}O_{19}$/α-Fe composites exhibited higher values of saturation

magnetization (Ms), remanent magnetization (Mr), and coercivity (Hc), reflecting their relatively stable domain structures. However, after 30 hours of high-energy milling, a substantial reduction in all three parameters was observed. For example, pure $BaFe_{12}O_{19}$ showed a decrease in Ms from 0.41 T to 0.07 T, and Hc dropped from 92.05 kA/m to 37.40 kA/m (Figure 3). Similarly, the $BaFe_{12}O_{19}$/α-Fe (99/1%) composite exhibited a reduction in Ms from 0.26 T to 0.09 T and in Hc from 99.22 kA/m to 45.53 kA/m.

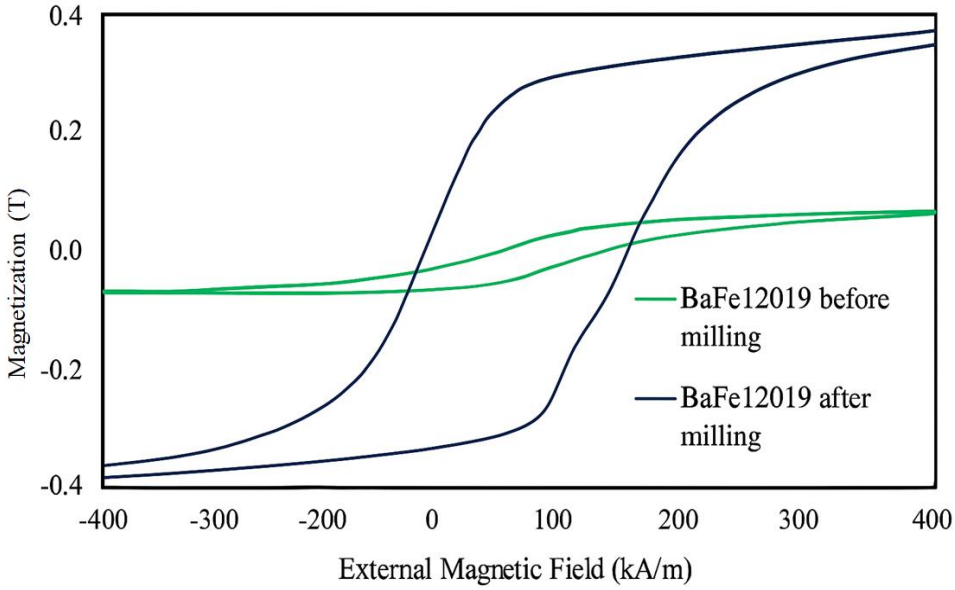

Figure 3: hysteresis curve of $BaFe_{12}O_{19}$ before and after milling for 30 hours

This decline can be attributed to crystallite size refinement into the nanometer regime, which introduces structural defects, surface disorder, and spin canting. While milling reduces long-range magnetic ordering, it enhances surface-to-volume ratios and creates conditions for exchange coupling between hard ($BaFe_{12}O_{19}$) and soft (α-Fe) magnetic phases. Similar reductions in magnetic strength due to extended milling have been reported in previous studies (Sharma et al., 2006; Liu et al., 2009). Thus, although prolonged milling reduces intrinsic magnetic properties, it provides a pathway to engineer nanocomposites with tailored exchange-coupling effects, making them promising candidates for applications requiring a balance between high coercivity and enhanced magnetization.

3.9 Analysis of the Magnetic Properties of $BaFe_{12}O_{19}$/α-Fe Composite Magnets

$BaFe_{12}O_{19}$/α-Fe composite magnets were synthesized both with and without 30 hours of milling at two different concentrations. Their magnetic properties were analyzed using a magnetograph, and the corresponding hysteresis curves are presented in Figure 4.

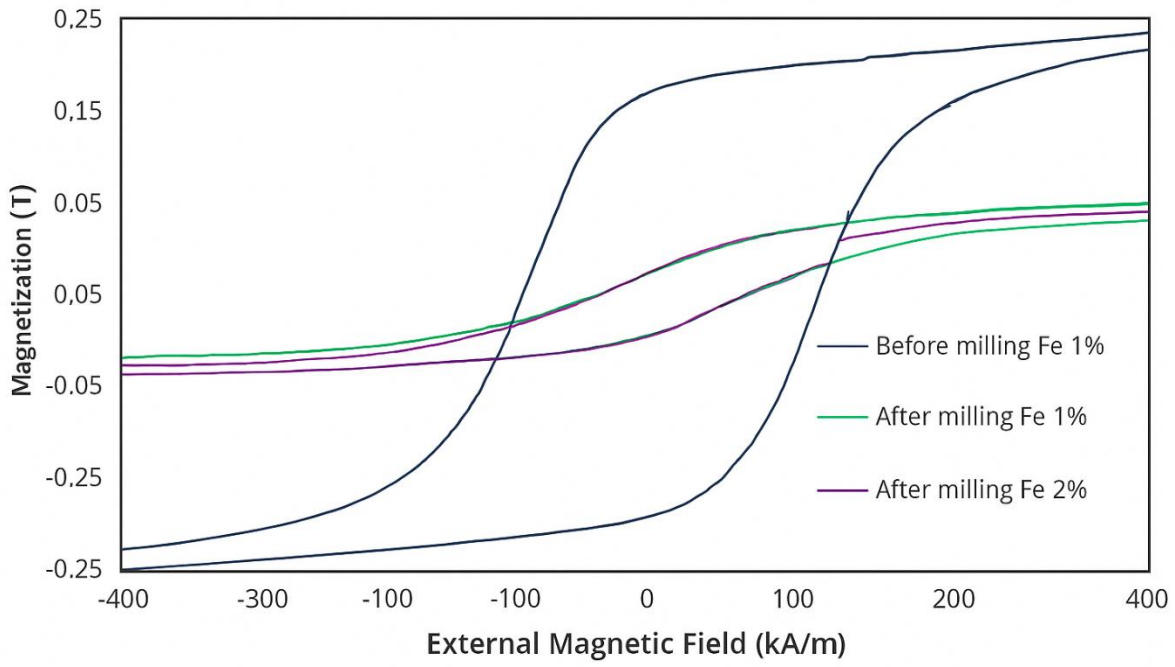

Figure 4: Magnetic hysteresis curve of BaFe12O19/α-Fe composite before and after milling for 30 hours

The results show that synthesis at two different concentrations led to an increase in remanent magnetization. This enhancement indicates that the remanent magnetization of $BaFe_{12}O_{19}$ can act as an internal bias field on α-Fe, thereby increasing the overall remanence and coercivity of the $BaFe_{12}O_{19}$/α-Fe composite magnets.

3.10 Particle Size Analysis (PSA) Results

The particle size distribution of $BaFe_{12}O_{19}$ before and after 30 hours of high-energy milling was examined using a particle size analyzer (PSA). The pristine $BaFe_{12}O_{19}$ powder exhibited an average particle size of approximately 20.26 µm, indicating its coarse, micrometer-scale nature. After the milling process, the particle size was significantly reduced, with crystallite size analysis from XRD confirming values in the nanometer range (~21–22 nm). The PSA data reflected a broader distribution after milling, suggesting the presence of both fine nanoparticles and some agglomerated clusters formed during repeated fracturing and cold welding. The pronounced reduction in size demonstrates the effectiveness of the mechanical alloying technique in achieving nanostructured powders. This refinement is advantageous, as nanosized $BaFe_{12}O_{19}$ provides larger surface area and enhanced potential for exchange coupling in composite and hybrid magnets, thereby influencing their overall magnetic performance.

4. Conclusion

This study successfully synthesized $BaFe_{12}O_{19}$/α-Fe nanocomposites through mechanical alloying, demonstrating the significant influence of prolonged milling on their structural and magnetic properties. High-energy ball milling for 30 hours refined $BaFe_{12}O_{19}$ crystallites to the nanometer scale (~21–22 nm), enhancing homogeneity but simultaneously introducing lattice strain and structural defects. As a result, both coercivity and saturation magnetization decreased compared to unmilled samples, consistent with earlier findings on nanostructured ferrites (Sharma et al., 2006; Liu et al., 2009). However, the incorporation of α-Fe provided a partial

enhancement of magnetic response through exchange coupling, reflecting the synergistic interaction between hard and soft magnetic phases (Ghasemi et al., 2012). The observed trade-off between structural refinement and magnetic strength highlights the need to optimize α-Fe content and milling duration for balanced performance. These results emphasize the novelty of exploring extended milling in $BaFe_{12}O_{19}$/α-Fe composites, bridging the gap between structural nanorefined ferrites and practical magnet design. Overall, the work contributes to the development of cost-effective, rare-earth-free nanocomposite magnets with tunable properties, suitable for advanced applications in high-density magnetic storage, energy-efficient devices, and permanent magnet technologies.

References

[1]. Auwal, I. A., Yahya, N., Hassan, O. H., Kamarudin, H., & Ismail, M. (2018). Influence of particle size on the structural and magnetic properties of $BaFe_{12}O_{19}$. *Ceramics International, 44*(7), 7884–7890. https://doi.org/10.1016/j.ceramint.2018.01.058

[2]. Chinnasamy, C. N., Jeyadevan, B., Tohji, K., & Shinoda, K. (2000). Magnetic properties of nanocrystalline $BaFe_{12}O_{19}$. *Journal of Applied Physics, 87*(9), 5196–5198. https://doi.org/10.1063/1.373386

[3]. Coey, J. M. D. (2010). *Magnetism and Magnetic Materials*. Cambridge University Press.

[4]. Cullity, B. D., & Graham, C. D. (2011). *Introduction to Magnetic Materials* (2nd ed.). Wiley-IEEE.

[5]. Ghasemi, A., Hossienpour, A., Liu, X., & Morisako, A. (2012). Exchange-coupled nanocomposite $BaFe_{12}O_{19}$/Fe. *Journal of Magnetism and Magnetic Materials, 324*(22), 3905–3911. https://doi.org/10.1016/j.jmmm.2012.06.056

[6]. Kodama, R. H. (1999). Magnetic nanoparticles. *Journal of Magnetism and Magnetic Materials, 200*(1–3), 359–372. https://doi.org/10.1016/S0304-8853(99)00347-9

[7]. Liu, J., Zeng, Y., Guo, C., Zhang, W., & Yang, X. (2009). Microwave sol-gel auto-combustion synthesis of nanocrystalline $BaFe_{12}O_{19}$. *Journal of Alloys and Compounds, 484*(1–2), 5–9. https://doi.org/10.1016/j.jallcom.2009.04.120

[8]. Martirosyan, K. S., Galstyan, E., & Luss, D. (2010). Carbon combustion synthesis of $BaFe_{12}O_{19}$ nanoparticles. *Journal of Applied Physics, 108*(11), 114317. https://doi.org/10.1063/1.3518367

[9]. Pullar, R. C. (2012). Hexagonal ferrites: A review of the synthesis, properties and applications. *Progress in Materials Science, 57*(7), 1191–1334. https://doi.org/10.1016/j.pmatsci.2012.04.001

[10]. Ramesh, R., & Coey, J. M. D. (2005). *Magnetism and Magnetic Materials*. Springer.

[11]. Sharma, P., Kumar, A., & Pant, R. P. (2006). Comparative study of $BaFe_{12}O_{19}$ powders prepared by mechanical alloying and conventional route. *Materials Chemistry and Physics, 98*(1), 104–107. https://doi.org/10.1016/j.matchemphys.2005.09.043

[12]. Skomski, R., & Coey, J. M. D. (1999). *Permanent Magnetism*. Institute of Physics Publishing.

[13]. Suryanarayana, C. (2001). Mechanical alloying and milling. *Progress in Materials Science, 46*(1–2), 1–184. https://doi.org/10.1016/S0079-6425(99)00010-9

[14]. Tenaud, P., Respaud, M., Snoeck, E., & Fert, A. (1998). Exchange coupling in ferrite–metal composites. *Journal of Applied Physics, 83*(11), 6260–6262. https://doi.org/10.1063/1.367714

[15]. Valenzuela, R. (2005). *Magnetic Ceramics*. Cambridge University Press.